InGaAs spin light emitting diodes measured in the Faraday and oblique Hanle geometries

**R Mansell[1a], J-B Laloë[1], S N Holmes[1,2], A Petrou[3],
I Farrer[1], G A C Jones[1], D A Ritchie[1] and C H W Barnes[1]**

[1]Department of Physics, Cavendish Laboratory, University of Cambridge, J.J. Thomson Avenue, Cambridge, CB3 0HE, U.K.

[2]Toshiba Research Europe Limited, Cambridge Research Laboratory, 208 Cambridge Science Park, Milton Road, Cambridge CB4 0GZ, United Kingdom

[3]Department of Physics, 239 Fronczak Hall, University at Buffalo, The State University of New York, Buffalo, NY14260, U.S.A.

Abstract

InGaAs quantum well light emitting diodes (LED) with spin-injecting, epitaxial Fe contacts were fabricated using an *in-situ* wafer transfer process where the semiconductor wafer was transferred under ultrahigh vacuum conditions to a metals growth chamber to achieve a high quality interface between the two materials. The spin LED devices were measured optically with applied magnetic fields in either the Faraday or the oblique Hanle geometries in two experimental set-ups. Optical polarizations efficiencies of 4.5 % in the Faraday geometry and 1.5 % in the Hanle geometry are shown to be equivalent. The polarization efficiency of the electroluminescence is seen to decay as the temperature increases although the spin lifetime remains constant due to an influence of the D'yakonov-Perel' spin scattering mechanism in the quantum well.

[a] rm353@cam.ac.uk

1

1. Introduction

High spin polarization devices are necessary for the successful development of semiconductor spintronics [1-3]. It has been suggested that by using the spin of the electron to control devices rather than the current, improvements in speed and energy efficiency of electronic devices can be obtained as well as allowing for quantum qubits to be designed [4,5]. Due to the difficulty of creating highly spin-polarized semiconductor materials at ambient temperature [6] one of the most promising routes is to combine highly polarized ferromagnetic metals as spin-injectors with non-magnetic semiconducting channels. Measuring the polarization across the interface between the polarized injector material and the semiconductor structure plays an important role in materials selection. The interface plays an essential role as evidenced by the fact that half-metallic materials (with bulk polarization approaching 100%) do not translate into equivalent high spin polarizations when combined with GaAs devices [7,8]. Fe spin-injecting contacts, with a bulk polarization of ~ 40%, have provided the highest spin-injection polarizations of all the simple metals. Fe is closely lattice matched to GaAs and the interface between these materials has been studied in depth [9-13]. However, standard growth procedures that involve removing the semiconductor wafer from the ultrahigh vacuum (UHV), add unwanted impurities at the interface with a magnetic contact. In the work presented here, the spin-polarization as a function of temperature using an Fe contact on an InGaAs quantum well LED device is investigated where the transfer between the III-V and metals growth chamber was carried out *in-situ* under strict UHV conditions [10,14]. Recent electrical spin-injection measurements on the Fe/MgO/GaAs combination have demonstrated that low defect levels at the MgO/GaAs interface can be achieved by in-situ wafer transfer [15].

The devices measured here were from two different experimental geometries, the Faraday [10] and the oblique Hanle geometry [14,16]. We show these to be equivalent in terms of the measured optical polarization efficiency. From the oblique Hanle measurements we extract the temperature dependence of the spin lifetime of recombining electrons, which fits a D'yakonov-Perel' model [17]. In section 2 we discuss the device growth and fabrication. In section 3, results from the two

optical techniques are presented. Section 4 is a discussion of the results and the main experimental findings with a final summary in section 5.

2. Device fabrication

The LEDs are molecular beam epitaxy (MBE) grown p-i-n junctions with a quantum well in the centre of the intrinsic region. The semiconductor structure consists of 15 nm n-$Al_{0.1}Ga_{0.9}As$ (5×10^{18} cm^{-3}) / 15 nm n-$Al_{0.1}Ga_{0.9}As$ (1×10^{18} cm^{-3}) / 100 nm n-GaAs (1×10^{18} cm^{-3}) / 100 nm GaAs/10 nm $In_{0.2}Ga_{0.8}As$ / 100 nm GaAs / 500 nm p-GaAs (5×10^{18} cm^{-3}) grown on a p-type (1×10^{18} cm^{-3}) GaAs substrate. This wafer has been used for previous studies [14,18] and has a heavily doped n-type layer at the surface that is designed to produce a narrow Schottky barrier with the Fe contact. The Schottky barrier provides a tunnelling contact that is required to maintain a high spin-polarization between materials that have different resistivities [19,20]. The sample was then transferred *in-situ* under UHV to a metals growth chamber with a base pressure of 2 x 10^{-10} mbar. A 5 nm thick epitaxial Fe layer was deposited at ambient substrate temperature at a rate of 0.03 nm/s. Finally, the wafer was capped with 5 nm of Au to protect the Fe layer from oxidation upon removal from the vacuum chamber, prior to device processing. The LED devices were wet etched into 200 μm by 100 μm mesa using standard optical lithography. The p-type contact was formed by low-temperature 180ºC annealed In-Zn with evaporated Ti-Au top bonding contacts. The magnetic Fe contact was characterized using magneto-optical Kerr effect (MOKE) magnetometry, to confirm the four-fold magnetic anisotropy expected from epitaxial growth of Fe on GaAs [18]. The in-plane cubic easy axis switching fields were ~ 1.5-1.7 mT.

3. Optical Measurements

The electroluminescence from the $In_{0.2}Ga_{0.8}As$ quantum well in the device, measured at 4 K with a constant current of 0.4 mA is shown in figures 1(a) and (b). The data is shown for +0.83 T, +0.003 T and -0.83 T applied magnetic field in the oblique Hanle configuration. For the data at applied fields

the two polarization states are shown, with figure 1(b) being a close-up of the peaks shown in figure 1(a). The designed quantum well e1-hh1 emission energy is around 1.32 eV, significantly lower than the peak seen here at around 1.40 eV, with a shoulder at 1.41 eV. However, the energy is too low to be associated with recombination in the bulk of the device [21]. Thickness variations across the semiconductor wafer that occur during MBE growth of the heterostructure layers can alter the dominance of where the emission originates from in these devices [14]. We also observe variation in the position of the quantum well peak across the wafer which may be due to indium segregation which can occur in such pseudomorphically strained layers [22] depending on the growth conditions. It is also noticeable that the emission varies between the data sets. This is likely to be due to the drift in the device temperature due to the relatively large current density required for emission.

The LEDs were measured in the Faraday geometry [10], where a perpendicular magnetic field, large enough to saturate the hard axis magnetization, is applied out-of-plane. A second system was used to measure the devices in the oblique Hanle geometry, where a small magnetic field is applied at an angle (ϕ) to the normal to the sample [7,14,16] to saturate the Larmor precession, $\Omega\tau_s \gg 1$, where Ω is the Larmor frequency and τ_s is the spin lifetime. In both cases the optical polarization efficiency of the measured light is defined as $P = \dfrac{I_+ - I_-}{I_+ + I_-}$, where I_+ (I_-) is the intensity of left (right)-hand polarized light.

Figure 2 shows the polarization of the emitted light as a function of magnetic field in the Faraday geometry (magnetic field parallel to the light **k** vector), with all points measured at 1.43 eV, the peak of the quantum well emission at zero magnetic field in this device. Whilst the emission is likely to shift in energy with applied perpendicular field this shift will be fairly small (~0.5 meV) due to the small g-factor of around 0.8 in these quantum wells [23]. The magnetic field acts to saturate the magnetization of the Fe film in the out-of-plane direction, which occurs at ~ 2.2 T. An optical polarization of ~ 4.5 % at 5 T is seen for the three different applied current levels. Due to the

optical selection rules in GaAs quantum wells [17], only the component of the spin angular momentum parallel to the confining direction of the well contributes to the polarization signal. As the Fe magnetization is rotated out-of-plane from the in-plane remanent state, the optical polarization increases until the Fe contact is saturated out-of-plane. Figure 2 shows that there is no strong dependence of polarization on the current (or applied bias) through the device. This is in contrast to polarization results from the same wafer with other processed mesas seen in reference 14. In those devices the emission came from the n-type GaAs region near the interface, and the strong bias dependence seen was attributed to changing the density of electrons filling the potential minimum created in the n^+ doping region of the device. Here the results indicate that the electron density in the quantum well is not strongly changing with bias across the junction.

Figure 3(a) shows the oblique Hanle effect optical polarization at 4 K with the Hanle curve fit to the peak of the polarization shown in Figure 3(b). The polarization measurements are an average of 19 points at each field, calculated from consecutive positive and negative polarization spectra in order to minimize the effects of the drift seen in figure 1. This drift may be responsible for the asymmetry in the polarization between the two field signs. We see two opposite polarizations, a positive peak at 1.395 eV and a negative peak at 1.405 eV. In the oblique Hanle geometry a magnetic field is applied at a fixed angle (φ) to the normal of the sample (in this case 60°). As the field is increased the spins tend to align with the magnetic field. The shape of the curve depends on the spin-polarization, spin lifetime and recombination lifetime of the spins in the quantum well. The circular polarization of the light directly gives the spin-polarization of the electrons (S_z) which is given by:

$$S_Z = S_{0Y} \frac{\tau_S}{\tau_S + \tau_R} \frac{(\Omega T_S)^2 \cos\phi \sin\phi}{1 + (\Omega T_S)^2}$$, where S_{0Y} is the initial spin-injection polarization, τ_s is the

spin scattering time, τ_R is the electron radiative lifetime, the spin lifetime (T_s) is defined as:

$T_s^{-1} = \tau_s^{-1} + \tau_R^{-1}$ and Ω is the Larmor precession frequency given by $\Omega = g * \frac{\mu_B}{\hbar} B$, with g* the

electron Landé g-factor, μ_B the Bohr magneton, $\hbar$ Planck's constant and **B** the applied magnetic

field. We then fit S_z from the optical polarization as a function of applied magnetic field. From the Hanle fit the spin lifetime in the device is extracted in addition to the spin-injection polarization in the quantum well. We use a g-factor in these fits of -0.8 taken from measurements on similar quantum wells [23]. Due to the quantum mechanical selection rules recombination of electrons with heavy holes and light holes gives opposite optical polarizations [17]. This may explain the negative polarization peak seen at higher energy. However, it would be expected that the light-hole peak was separated by around 50 meV from the heavy-hole peak [24], rather than the 10 meV seen here.

In figure 4 the quantity $S_{0Y}.T_s/\tau_R$ is plotted on the left-hand axis versus temperature, where $S_{0Y}.T_s/\tau_R$ is the optical polarization of the electrons in the quantum well. This is the quantity directly measured in the Faraday geometry and the quantity extracted from the Hanle equation from the geometry of the measurement. This is the polarization after degradation from transit through the device and more importantly, the time spent in the quantum well. Transit through the device will account for a few ps whilst the decay time in the well will be > 100 ps [25]. The measured spin lifetime, T_s, will have contributions from both the transit through the device and the time in the quantum well. At low temperature there is a good agreement between the two experimental procedures.

This method can also be used to extract the spin-polarization across the interface if T_s, the spin lifetime, which comes from the Hanle fit, and τ_R, the radiative lifetime, which needs to be determined separately, are known. Using time-resolved photoluminescence on an equivalent undoped sample the electron lifetime was determined as 400 ps at 4 K. This allows the interfacial injection polarization, S_{0Y}, to be estimated as 50 ± 20 % at 4 K, which is in line with other measurements [11,12,26] and the expected spin-polarization of Fe [27].

Oblique Hanle effect measurements were made at temperatures from 4 K to 300 K and Hanle curves were fitted to give the spin lifetime and optical polarization in the well ($S_{0Y}.T_s/\tau_R$) over the temperature range as shown in Figure 4. The 30 to 40 ps spin lifetime has very little dependence on temperature. This flat temperature dependence is similar to that previously seen in other quantum

well systems and indicates the dominance of the D'yakonov-Perel' mechanism over the whole temperature range [17,28]. It also shows that the spin lifetime is dominated by the quantum well rather than transit through the device, as bulk spin relaxation under the D'yakonov-Perel' mechanism gives a temperature (T) dependence of $T^{-3/2}$ if the momentum scattering is dominated by charged impurity scattering as would be expected from the n-type doped transit region [29]. The polarization in the quantum well is seen to decrease with temperature from the low temperature peak of ~ 4.5 % to ~ 1 % at ambient temperature. Since we see constant T_s in the device across the temperature range, this decrease in polarization is likely to be due to an increase in the radiative lifetime of the electrons at higher temperatures [30].

4. Discussion

The similar polarizations seen in the Faraday and oblique Hanle geometries show that there is no dependence of the relative orientation of the magnetization with the interface that would manifest as a tunnelling anisotropic magnetoresistance (TAMR) signal [31]. Whilst large TAMR effects have been seen in specially designed samples, for Fe/GaAs interfaces the numbers are quite small, < 1 % of the total signal [32], which is well within the errors of this experiment. These effects may become more pronounced if Heusler alloys [33], or synthetic multilayers, are used to create spin-injecting elements in spintronic devices. The interfacial Schottky barrier in GaAs, due to the dominance of conduction at the Γ-point in k-space is unlikely to have a large TAMR effect.

Whilst the results from both experiments are consistent, it is notable that the polarizations are small. In similar systems optical polarizations of 30 % have been measured [11,12,26]. The lower value seen here is consistent with the relatively small spin lifetimes that we extract from the Hanle effect. In comparison, in bulk GaAs channels lifetimes > 1 ns have been measured [34]. The reduction in spin lifetime is likely to be due to an excess number of dopants in the sample. Reference [35] has shown that higher doped p-i-n junctions have reduced spin efficiency due to the creation of a population of unpolarized carriers in the quantum well. This gives rise to extra

electron-electron scattering and means that not all of the recombining electrons come from the polarized injecting source. The samples studied have considerably more doping than the high doped LEDs in reference [35]. Whereas in reference [35] devices consist of a highly doped injector followed by 150 nm of material doped at 1×10^{17} cm^{-3}, the devices studied here have 100 nm of 1×10^{18} cm^{-3} after the injector in these samples, a factor of 6 higher. An excess of electrons in the well is also consistent with a D'yakonov-Perel' scattering mechanism, which is dominant for doped n-type semiconductors [36,37]. The high doping in these samples was also partly responsible for the creation of a potential minimum near the Schottky barrier in devices made from the same semiconductor wafer, albeit due to growth variations across the wafer. Recombination from this region was shown to be highly dependent on the sample bias, which would cause a change in the unpolarized electron population at this minimum [14]. The large carrier density in the well would also favour band-to-band rather than excitonic recombination [30].

5. Summary

InGaAs-based spin-LEDs with in-situ grown Fe spin-injectors were measured in both the Faraday and Hanle geometries. In the Faraday geometry a polarization of 4.5 ± 1 % was measured at 4 K, which was shown to be consistent with a peak optical polarization of 1.5 % measured in the Hanle geometry. The Hanle effect experimental data also provided the spin lifetime as a function of temperature, which was seen to remain constant at around 30 to 40 ps from 4 K to ambient temperature, consistent with a D'yakonov-Perel' type model for a two-dimensional system. The low electron spin-polarization seen in these samples can be explained by an excess of n-type dopants in the p-i-n junction which leads to population of the quantum well by unpolarized electrons.

Here we see that although most of the effort in semiconductor spintronics devices has been on improving the spin-injecting contact, optimization of the semiconductor is also required. Conventional band structure modelling of the semiconductor devices is not able to capture the full range of effects that may reduce the spin-polarisation efficiency in the semiconductor, however in-

situ wafer transfer is essential in reducing the impact of defects and impurities at the interface as a starting point.

References

[1] S. Datta and B. Das, Appl. Phys. Lett. **56** 665 (1990)

[2] Hyun Cheol Koo, Jae Hyun Kwon, Jonghwa Eom, Joonyeon Chang, Suk Hee Han, and Mark Johnson, Science **325**,1515 (2009)

[3] A. T. Hanbicki, B. T. Jonker, G. Itskos, G. Kioseoglou, A. Petrou, Appl. Phys. Lett. **80**, 1240 (2002)

[4] D. Loss and D. P. DiVincenzo, Phys. Rev. A **57**, 120 (1998)

[5] S. A. Wolf, D. D. Awschalom, R. A. Buhrman, J. M. Daughton, S. von Molnar, M. L. Roukes, A. Y. Chtchelkanova and D. M. Treger, Science **294**, 1488 (2001)

[6] T. Dietl, Nat. Mater. **9**, 965 (2010)

[7] M. C. Hickey, C. D. Damsgaard, S. N. Holmes, I. Farrer, G. A. C. Jones, D. A. Ritchie, C. S. Jacobsen, J. B. Hansen and M. Pepper, Appl. Phys. Lett. **92**, 232101 (2008)

[8] R. Mansell , J.-B. Laloë , S. N. Holmes , P. K. J. Wong , Y. B. Xu , I. Farrer , G. A. C. Jones , D. A. Ritchie and C. H. W. Barnes, J. Appl. Phys. **108**, 034507 (2010)

[9] S. Honda, H. Itoh, J. Inoue, H. Kurebayashi, T. Trypiniotis, C. H. W. Barnes, A. Hirohata, and J. A. C. Bland, Phys. Rev. B **78**, 245316 (2008)

[10] X. Lou, C. Adelmann, S. A. Crooker, E. S. Garlid, J. Zhang, K. S. M. Reddy, S. D. Flexner, C. J. Palmstrøm, and P. A. Crowell: Nat. Phys. **3**, 197 (2007)

[11] George Kioseoglou, Aubrey T. Hanbicki, James M. Sullivan, Olaf M. J. van 't Erve, Connie H. Li, Steven C. Erwin, Robert Mallory, Mesut Yasar, Athos Petrou & Berend T. Jonker, Nat. Mater. **3**, 799 (2004)

[12] A. T. Hanbicki, O. M. J. van't Erve, R. Magno, G. Kioseoglou, C. Li, B. T. Jonker, G. Itskos, R. Mallory, M. Yasar, A. Petrou, Appl. Phys. Lett. **82**, 4092 (2003)

[13] A. Cabbibo, J.R. Childress, S.J. Pearton, F. Ren, and J.M. Kuo, Journal of Vacuum Science & Technology A, 15, 1215-1219 (1997)

[14] M. C. Hickey, S. N. Holmes, T. Meng, I. Farrer, G. A. C. Jones, D. A. Ritchie, and M. Pepper

Phys. Rev. B **75**, 193204 (2007)

[15] Seong Hoon Shim, Hyung-jun Kim, Hyun Cheol Koo, Yun-Hi Lee and Joonyeon Chang, Appl. Phys. Lett. **107**, 102407 (2015)

[16] V. F. Motsnyi, P. Van Dorpe, W. Van Roy, E. Goovaerts, V. I. Safarov, G. Borghs, and J. De Boeck, Phys. Rev. B **68**, 245319 (2003)

[17] M. I. Dyakonov and V. I. Perel, Optical Orientation, vol. 8 of Modern Problems in Condensed Matter Science, Amsterdam: North-Holland (1984)

 [18] R. Mansell, J.-B. Laloe, S. N. Holmes, I. Khan, M. Yasar, A. Petrou, I. Farrer, G. A. C. Jones, D. A. Ritchie and J. A. C. Bland, IEEE Transactions on Magnetics **44**, 2666 (2008)

[19] G. Schmidt, D. Ferrand, L. W. Molenkamp, A. T. Filip and B. J. van Wees, Phys. Rev. B **62**, R4790(R) (2000)

[20] E. I. Rashba, Phys. Rev. B **62**, R16267 (2000)

[21] G. Bacquet, F. Hassen, C. Fontaine, W.S. Hobson, and S.J. Pearton, Solid-State Electronics, **38** 1523 (1995)

[22] H. Yu, C. Roberts, and R. Murray, Ray, Appl. Phys. Lett. **66**, 2253 (1995)

[23] B. Kowalski, V. Zwiller, C. Wiggren, P. R. Varekamp, M. S. Miller, M. E. Pistol, P. Omling, and L. Samuelson, Japanese Journal of Applied Physics **37**, 4272 (1998)

[24] G. Ji, D. Huang, U.K. Reddy, T.S. Henderson, R. Houdré and H. Morkoç, Journal of Applied Physics, **62**, 3366 (1987)

[25] G. Bacher, C. Hartmann, H. Schweizer, T. Held, G. Mahler, and H. Nickel, Phys. Rev. B **47**, 9545 (1993)

[26] O. M. J. van 't Erve, G. Kioseoglou, A. T. Hanbicki, C. H. Li, and B. T. Jonker, Appl. Phys. Lett. **89**, 072505 (2006)

[27] R. J. Soulen, J. M. Byers, M. S. Osofsky, B. Nadgorny, T. Ambrose, S. F. Cheng, P. R. Broussard, C. T. Tanaka, J. Nowak, J. S. Moodera, A. Barry and J. M. D. Coey, Science **282**, 85 (1998)

[28] A. Malinowski, R. S. Britton, T. Grevatt, R. T. Harley, D. A. Ritchie, and M. Y. Simmons,

Phys. Rev. B **62**, 13034 (2000)

[29] I. Zutic, J. Fabian and S. Das Sarma, Reviews of Modern Physics **76**, 323 (2004)

[30] T. Matsusue and H. Sakaki, Appl. Phys. Lett. **50**, 1429 (1987)

[31] C. Rüster, C. Gould, T. Jungwirth, J. Sinova, G. M. Schott, R. Giraud, K. Brunner, G. Schmidt, and L. W. Molenkamp, Phys. Rev. Lett. **94**, 027203 (2005)

[32] Tetsuya Uemura, Yosuke Imai, Masanobu Harada, Ken-ichi Matsuda and Masafumi Yamamoto, Appl. Phys. Lett. **94**, 182502 (2009)

[33] Tetsuya Uemura, Masanobu Harada, Ken-ichi Matsuda and Masafumi Yamamoto, Appl. Phys. Lett. **96**, 252106 (2010)

[34] J. M. Kikkawa and D. D. Awschalom, Phys. Rev. Lett. **80**, 4313 (1998)

[35] M. Yasar, R. Mallory, A. Petrou, A. T. Hanbicki, G. Kioseoglou, C. H. Li, O. M. J. van't Erve, and B. T. Jonker, Appl. Phys. Lett. **94**, 032102 (2009)

[36] M. Q. Weng, M. W. Wu and L. Jiang, Phys. Rev. B **69**, 245320 (2004)

[37] W. J. H. Leyland, G. H. John, R. T. Harley, M. M. Glazov, E. L. Ivchenko, D. A. Ritchie, I. Farrer, A. J. Shields and M. Henini, Phys. Rev. B **75**, 165309 (2007)
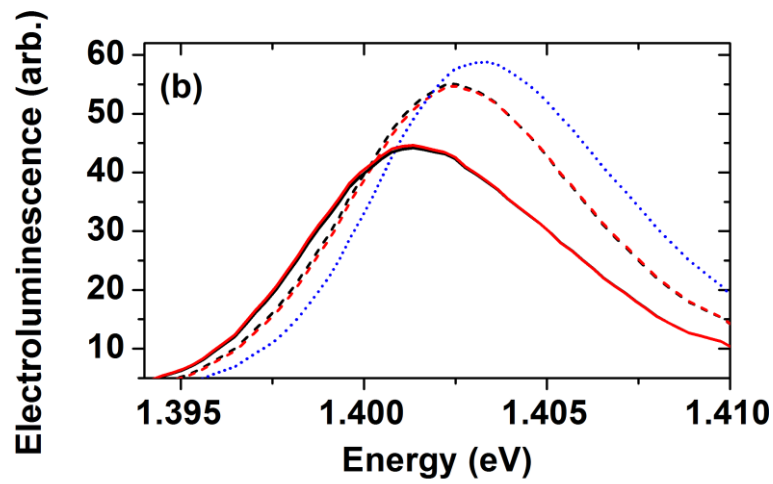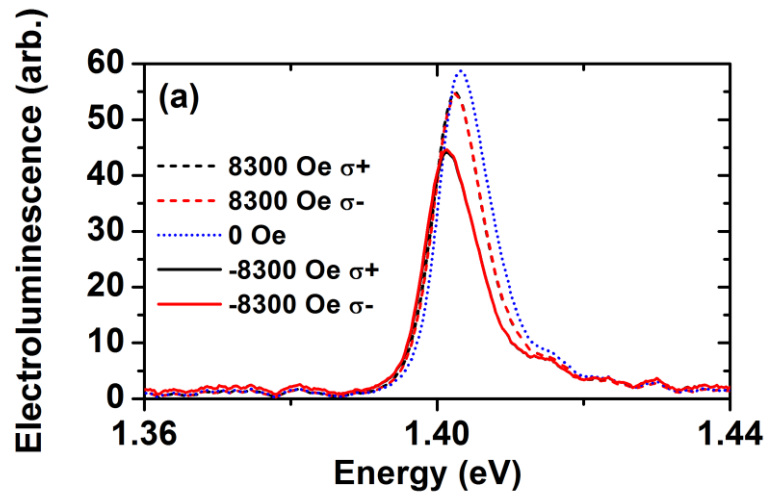
Figure captions

Figure 1. (a) Electroluminescence signal at 4 K with a current of 0.4 mA, showing data at +0.83 T, +0.003 T and -0.83 T in the oblique Hanle orientation, with the two light polarizations for the data taken with applied fields. (b) Detail around the main peaks in (a).

Figure 2. Faraday geometry polarization data at 7 K measured at 1.432 eV with currents from 0.1 to 5 mA.
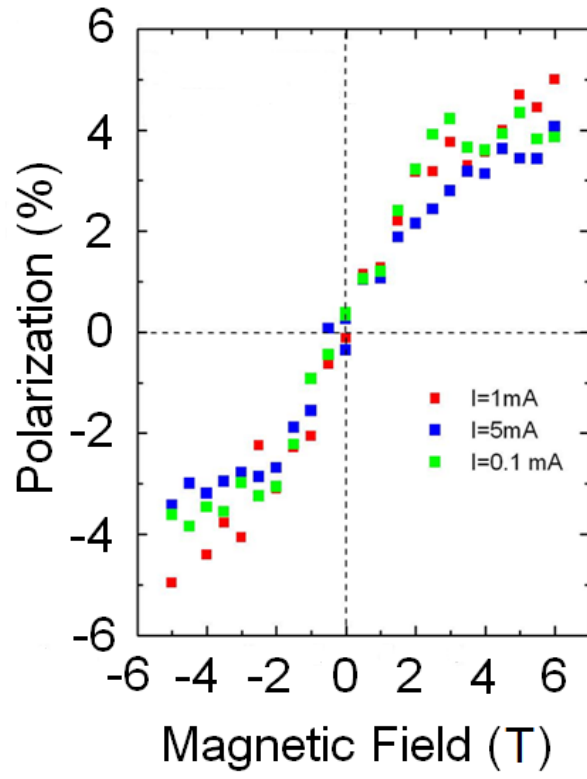
Figure 3. (a) Optical polarization measured as a function of applied magnetic field in the Hanle geometry at 4.2 K with 0.4 mA current. (b) The Hanle curve experimental data points and fits at 1.397 eV, for the heavy hole emission peak.

Figure 4. The temperature dependence of the extracted quantity, $S_{0y}T_s/\tau_R$ for the Hanle measurement (blue) and the temperature dependence of spin lifetime, T_s (in red). A single (black) data point at 7 K shows the Faraday measurement of $S_{0y}T_s/\tau_R$.
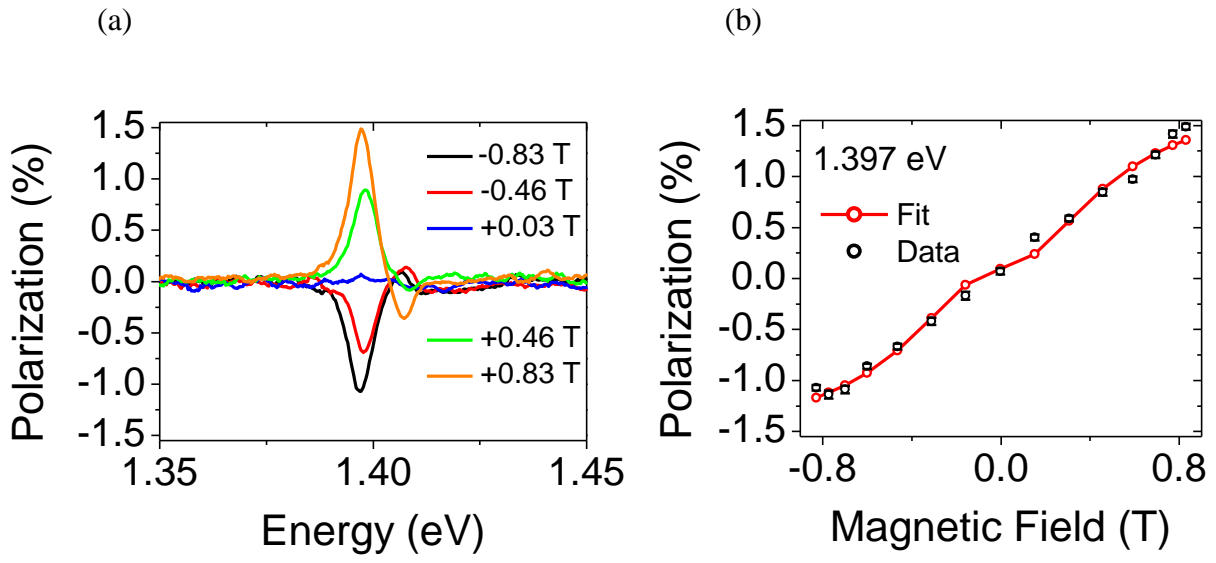
Figure 1

Figure 2

Figure 3

(a)

(b)

Figure 4